Influence of Solar Heating and Precipitation Scavenging on the Simulated Lifetime of Post–Nuclear War Smoke

Abstract. *The behavior of smoke injected into the atmosphere by massive fires that might follow a nuclear war was simulated. Studies with a three-dimensional global atmospheric circulation model showed that heating of the smoke by sunlight would be important and might produce several effects that would decrease the efficiency with which precipitation removes smoke from the atmosphere. The heating gives rise to vertical motions that carry smoke well above the original injection height. Heating of the smoke also causes the tropopause, which is initially above the smoke, to re-form below the heated smoke layer. Smoke above the tropopause is physically isolated from precipitation below. Consequently, the atmospheric residence time of the remaining smoke is greatly increased over the prescribed residence times used in previous models of nuclear winter.*

ROBERT C. MALONE
LAWRENCE H. AUER
GARY A. GLATZMAIER
MICHAEL C. WOOD
Earth and Space Sciences Division, Los Alamos National Laboratory, Los Alamos, New Mexico 87545
OWEN B. TOON
Space Science Division, NASA Ames Research Center, Moffett Field, California 94035

The possibility that a large quantity of smoke might be injected into the atmosphere by massive fires after a nuclear war was proposed by Crutzen and Birks (*1*). This smoke, when spread around the globe, could absorb much of the incoming solar radiation, diminishing the solar flux at the earth's surface and causing the continental surface temperatures to be lowered, the "nuclear winter" effect found by Turco *et al.* (*2*). The severity and duration of cooling depend on the injected mass and physical characteristics of the smoke and on the manner in which the smoke is subsequently heated by sunlight, redistributed by the winds, and removed from the atmosphere by scavenging processes (*2, 3*). These processes, particularly smoke removal by precipitation, are complex and can be treated only approximately in three-dimensional climate models. We conducted computer modeling studies that treat these processes and their mutual interactions. Our results are qualitatively different from those of previous studies and may modify our understanding of nuclear winter.

In initial studies of nuclear winter, smoke was not transported (*2–4*). Smoke removal was either prescribed by the use of observed aerosol residence times in the unperturbed atmosphere (*2, 3*) or ignored (*4*). These studies led to the idea that smoke injected in the troposphere (*5*) would remain there, where it would be subject to removal by rainfall and would have a lifetime of only weeks.

Subsequent two-dimensional studies of the influence of solar heating on the vertical transport of smoke (*6*) showed that smoke could be driven into the stratosphere. Our three-dimensional calculations and those of Thompson (*7*) support this interpretation. In addition, the changes in atmospheric structure, precipitation, and scavenging that are induced by solar heating of smoke can be computed by our model. These important changes cannot be accounted for in models with prescribed removal rates.

Our results illustrate the competition that would exist between removal of smoke by precipitation and heating of smoke by sunlight. Solar heating of smoke would have two consequences, both of which would tend to separate it from precipitation and thereby increase its lifetime in the atmosphere. The first of these is vertical transport induced by the heating, which moves smoke-filled air upward, with compensating subsidence elsewhere. The second is downward displacement of the tropopause; since precipitation is confined below this level, the volume of atmosphere in which scavenging occurs would be reduced. For injections in the Northern Hemisphere during summer, when solar heating is maximum, the lifetime of smoke is greatly increased, qualitatively changing the duration of the nuclear-winter effect. In winter, a significant though smaller increase in lifetime is found.

To study the interactions among the transport, heating, and scavenging of smoke, we augmented the capabilities of a general circulation model (*8*) to include each of these effects (*9*). The coarse horizontal resolution of this model precludes investigation of potentially important but poorly understood transport and removal processes at scales of less than 500 to 1000 km.

The behavior of 170×10^9 kg (*3*) of smoke injected into the atmosphere (*10*) was simulated for 40 days. January and July conditions were used to examine the seasonal dependence of atmospheric effects. Sensitivity to the vertical injection distribution was examined by comparing a "low" (2 to 5 km) injection and an "NAS" injection [constant density of smoke between 0 and 9 km (*3*)]. In addition to computer experiments with interactive smoke, which absorbs solar radiation, other experiments were conducted with a passive tracer, which does not. In a given experiment, smoke or tracer is transported by the model winds and scavenged by model-predicted precipitation. Unlike smoke, the passive tracer has no influence on the evolution of the simulated atmosphere.

The importance of the vertical transport induced by solar heating of the smoke-filled atmosphere is illustrated in Fig. 1 for July conditions. The concentration of interactive smoke is contrasted with that of a passive tracer. By the third week, part of the smoke cloud has been carried upward by currents generated by the intense solar heating, but much of the smoke low in the atmosphere has been

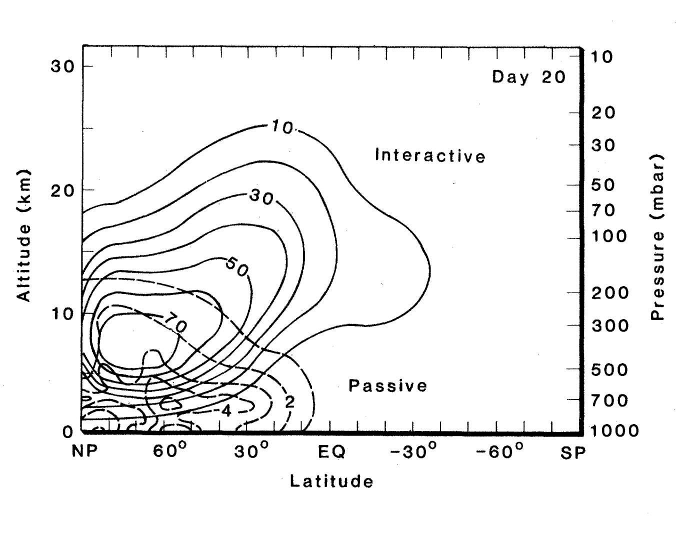

Fig. 1. Longitudinally averaged mass mixing ratios for July conditions at day 20. The dashed contours apply to passive tracer, the solid contours to interactive smoke. In each case, 170×10^9 kg of material was injected (*10*) between 2 to 5 km. The contours of mixing ratio are labeled in units of 10^{-9} g of material per gram of air. Note the much greater reduction in concentration of passive tracer compared to smoke. EQ, equator; NP, North Pole; and SP, South Pole.

Fig. 2. The relative positions of the modified tropopause (heavy dashed line) and region of significant precipitation (cross-hatched region below the tropopause), both averaged over days 15 to 20, and the smoke distribution at day 20 (stippled area above the tropopause) for 170×10^9 kg injected (*10*) between 0 and 9 km in July. Darker stippling indicates greater smoke loading; the smoke contour intervals correspond to mixing ratios of 10, 40, and 70×10^{-9} g of smoke per gram of air.

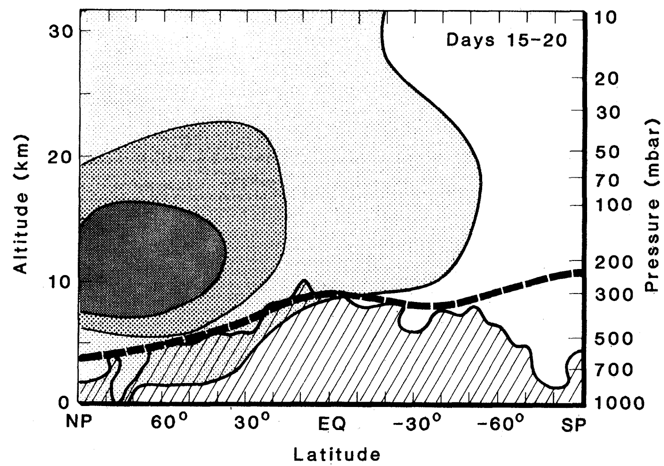

removed by precipitation. Thompson (*7*) found qualitatively similar smoke lofting in a model that ignores smoke removal. The passive tracer leads to a different result. Since it is not heated by the sun, it remains concentrated near its original injection height and is rapidly scavenged.

The second effect of solar heating of smoke is that the tropopause, which separates the precipitation-bearing troposphere from the stably stratified layer above (*11*), disappears in the simulation from its normal altitude (9 to 13 km) and re-forms at a much lower position below the level of maximum heating. Precipitation is confined below this altered tropopause (Fig. 2), thus smoke above the tropopause is not directly affected by precipitation. Note that smoke above the tropopause is transported into the Southern Hemisphere by a global Hadley-like circulation.

The vertical transport of smoke and the change in atmospheric structure combine to greatly enhance the simulated lifetime of smoke. The amount of smoke remaining in the global atmosphere is shown as a function of time in Fig. 3. Since the influence of solar heating develops gradually, a large fraction of the smoke is scavenged by precipitation during the first few weeks. After that, smoke above the new tropopause is removed more slowly, due to its increasing isolation from precipitation.

The July model (Fig. 3) shows that about two-thirds of the injected smoke has been removed by day 40, despite the reduced scavenging after 2 weeks. Only a slight decrease in lifetime is predicted when the smoke is injected between 2 and 5 km instead of between 0 and 9 km; at day 40, the $1/e$ residence time (*12*) of the remaining smoke is about 5 and 6 months, respectively. This residence time agrees well with the time required for particles to fall (*10*) from the concentration maximum near 10 km to the tropopause near 5 km (Fig. 2), where they can be rapidly scavenged by precipitation. This slow removal of smoke at late times causes significant cooling of the continents in the Northern Hemisphere to persist through day 40 of the simulation. If spread uniformly over the globe, the remaining smoke mass would produce an absorption optical depth of about 0.2, corresponding to an 18 percent reduction of light from the sun overhead. After the first week, our computed optical depths are considerably smaller than those obtained by Thompson (*7*) because smoke is removed in our simulations.

For smoke injected in January, when the solar flux in the Northern Hemisphere is relatively small, heating is reduced and only weak vertical transport

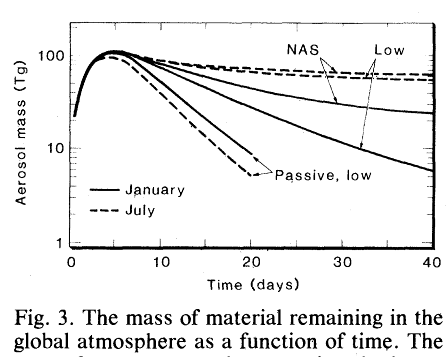

Fig. 3. The mass of material remaining in the global atmosphere as a function of time. The upper four curves apply to smoke, the lower pair to passive tracer. Solid and dashed curves indicate January and July conditions, respectively. Labels indicate low (2 to 5 km) and NAS (0 to 9 km) injections. The slopes of the passive tracer curves at late times yield $1/e$ residence times (*12*) of 5 to 6 days; these agree well with observed residence times of aerosols in the lower troposphere (*9, 13*).

and minor atmospheric alteration occur in the model. In this case, smoke remains lower in a less perturbed atmosphere and is removed faster. By day 40 (Fig. 3) the model shows that 85 to 95 percent of the smoke has been removed. However, even in January, the effects of solar heating on scavenging are important, as can be seen by comparing the smoke and passive tracer curves. There is a greater sensitivity to the vertical injection distribution in January. At day 40, the $1/e$ residence time is only about 2 weeks for the interactive low case but about 1.5 months for the NAS case.

The amount of smoke that would be produced by a nuclear war is not known (*3*). In both winter and summer, absorption of sunlight decreases as the mass of injected smoke decreases. Consequently, the influence of solar heating diminishes, and smoke is removed more efficiently by precipitation. For smoke masses of 5, 20, 60, 170, and 500×10^9 kg injected with July conditions and the NAS profile, the fractional mass remaining at day 40 in the simulations is about 7, 22, 35, 36, and 28 percent, respectively. The decrease at high smoke loadings is due to shielding of low-lying smoke in opaque smoke clouds; this inhibits lofting and favors scavenging.

The increase in smoke lifetime due to solar heating implies an increased duration of the nuclear winter effect. For a 170×10^9 kg smoke injection in July, surface air temperature reductions of 15° to 25°C relative to normal are predicted for interiors of Northern-Hemisphere continents during the first few weeks. Although much smoke is scavenged (Fig. 3), enough remains at the end of the calculation (40 days) for reductions of 5° to 15°C to persist. In January, reductions of 15°C or less are predicted during the first few weeks, but the faster removal of smoke permits temperatures to return to normal more quickly than in July. Smaller climate effects, as well as shorter smoke lifetimes, are found for smaller amounts of injected smoke (*9*).

References and Notes

1. P. J. Crutzen and J. W. Birks, *Ambio* **11**, 114 (1982).
2. R. P. Turco *et al.*, *Science* **222**, 1283 (1983).
3. National Academy of Sciences, *The Effects of the Atmosphere of a Nuclear Exchange* (National Academy Press, Washington, D.C., 1985).
4. C. Covey, S. H. Schneider, S. L. Thompson, *Nature (London)* **308**, 21 (1984).
5. Temperature decreases upward in the troposphere, the lowest part of the atmosphere. Above the tropopause in the stratosphere, temperature increases upward. Precipitation occurs in the troposphere, but not above the tropopause.
6. R. M. Haberle *et al.*, *Geophys. Res. Lett.* **12**, 405 (1985).
7. S. L. Thompson, *Nature (London)*, in press.
8. E. J. Pitcher *et al.*, *J. Atmos. Sci.* **40**, 580 (1983); V. Ramanathan *et al.*, *ibid.*, p. 605; R. C. Malone *et al.*, *ibid.* **41**, 1394 (1984).

9. For details on the model and validation studies, and more information on the climate effects for various smoke masses, see R. C. Malone *et al.*, *J. Geophys. Res.*, in press.
10. Smoke or passive tracer is injected over the United States, Europe, and the western Soviet Union at a rate that is maximum at day 0 and decreases linearly to 0 at day 7; half the mass is injected during the first 2 days. We take the solar absorption coefficient of smoke to be 2 m^2/g (*3*). Both precipitation scavenging and gravitational sedimentation are treated (*9*). We assume a particle radius of 1 μm in calculating the gravitational fall velocity, which is about 3×10^{-4} m/sec at an altitude of 10 km (*13*).
11. In the unperturbed atmosphere this stably stratified layer is the normal stratosphere, but in the perturbed atmosphere, it is the heated smoke layer itself.
12. The $1/e$ residence time is the time required for the mass of smoke to decrease further by a factor of $1/e$ ($e \simeq 2.72$).
13. H. R. Pruppacher and J. D. Klett, *Microphysics of Clouds and Precipitation* (Reidel, Boston, 1978).
14. We thank E. Jones, H. Bethe, R. Turco, T. Ackerman, J. Hyman, R. Haberle, D. Westphal, and D. Bacon for helpful discussions, and A. Kron for drafting the figures. Supported by Department of Energy contract W-7405-ENG-36 and Defense Nuclear Agency task codes S99QMXBB-56 and S99QMXBB-58.

3 June 1985; accepted 30 July 1985

Deletion in Chromosome 11p Associated with a Hepatitis B Integration Site in Hepatocellular Carcinoma

Abstract. *Hepatitis B virus (HBV), a virus with known carcinogenic potential, integrates into cellular DNA during long-term persistent infection in man. Hepatocellular carcinomas isolated from viral carriers often contain clonally propagated viral DNA integrations. As small chromosomal deletions are associated with several types of carcinomas, the occurrence of chromosomal deletions in association with HBV integration in hepatocellular carcinoma was studied. HBV integration was accompanied by a deletion of at least 13.5 kilobases of cellular sequences in a human hepatocellular carcinoma. The viral DNA integration and deletion of cellular sequences occurred on the short arm of chromosome 11 at location 11p13-11p14. The cellular sequences that were deleted at the site of HBV integration were lost from the tumor cells, leaving only a single copy of the remaining cellular allele.*

C. E. Rogler
M. Sherman
C. Y. Su
D. A. Shafritz
Department of Medicine, Albert Einstein College of Medicine, Bronx, New York 10461
J. Summers
Institute for Cancer Research, Philadelphia, Pennsylvania 19111
T. B. Shows
Department of Human Genetics, Roswell Park Memorial Institute, Buffalo, New York 14263
A. Henderson
Department of Biological Sciences, Hunter College, City University of New York, New York 10021
M. Kew
Department of Medicine, University of Witwatersrand, Johannesburg 2001, South Africa

Hepatitis B virus (HBV) and Woodchuck hepatitis virus (WHV), two of four members of the hepadna virus family (*1*), exhibit characteristics associated with oncogenic viruses. Chronic infection with either of these viruses incurs a high risk of hepatocellular carcinoma (approximately 40 percent for HBV and 90 percent for WHV) (*2–4*). The finding of viral integrations in genomic DNA prepared from primary hepatomas of chronically infected humans and woodchucks (*3, 5–7*) has suggested a possible role of these integrations in hepatocarcinogenesis. Integration can occur at variable sites for both the cellular and viral DNA's (*5, 8–13*), similar to findings observed for integrated SV40 DNA in transformed eukaryotic cell lines (*14, 15*). However, in the case of HBV and WHV, an oncogene has not yet been identified (*8–10*).

In addition to searching for common integration sites, we have investigated the possibility that HBV integration may function in hepatocellular carcinoma by causing chromosomal deletions or translocations. The present study reports that a large genomic DNA deletion is associated with an HBV integration isolated from a primary liver tumor. We also demonstrate that the deleted sequences are lost from the tumor cells, leaving only a single copy of the normal cellular allele.

DNA was obtained from tumor HL70 (*6*), a postmortem specimen of primary hepatocellular carcinoma from a chronic HBV surface antigen (HBsAg) carrier (*6*). A Southern blot of Hind III-digested HL70 DNA, hybridized with cloned HBV DNA, showed three bands containing HBV DNA sequences. Two of these integrations were cloned into the Hind III site of bacteriophage Charon 30 (*5*). The restriction endonuclease map of one of the clones, HL70-3, is shown in Fig. 1A. This Hind III fragment was 10 kilobases (kb) in length and contained a 2.8-kb segment of integrated HBV DNA. The coding sequences for the entire X gene (function unknown) and the viral core antigen gene (HBcAg) of HBV were present as integrated sequences. The location of these genes in the clone (Fig. 1A) spans the 1.2-kb HBV DNA segment that contains two Ava I sites. As complete cloned HBV genomes contain only one Eco RI site (*16*), the presence of two Eco RI sites in the integrated HBV sequence could be due to various causes, including the generation of a new Eco RI site by base mutation or a rearrangement of viral sequences resulting in duplication of the Eco RI site. The latter is more likely as a duplication would be consistent with the structure of integrated viral DNA that we and others have observed (*5, 8, 11*). The restriction map also indicates that HBsAg gene sequences are present in this clone; however, on the basis of the published restriction endonuclease map of HBV (*16*), the entire surface antigen gene is not present.

Two restriction fragments, corresponding to a portion of the left-end cellular sequence (pS8-1) and the right-end cellular sequence (HL70-3-4) of clone HL70-3 were identified and shown to be free of highly repeated DNA (they did not hybridize to a probe made from total human DNA). These sequences were subcloned into plasmid vectors. The subclones were used as probes to construct a restriction endonuclease map of cellular DNA sequences at the HBV integration site in the original tumor HL70, and cellular DNA sequences comprising the normal homologous cellular allele. The probes hybridized to two bands in the tumor DNA and one band in the normal human DNA (Fig. 1B). The band unique to tumor DNA represents the DNA that had been modified by HBV integration.

The sizes of those restriction fragments that corresponded to the normal and tumor DNA sequences hybridizing to each flanking probe and the known restriction map of clone HL70-3 were used to construct a restriction map of the normal and tumor loci (Fig. 1C). This method allowed us to map only from the probe site to the first restriction endonuclease site outside the probe in either direction for any particular enzyme. The boundaries of the deleted region represent the HBV integration site. The restriction map of the normal cellular sequences extending within the deleted region 5.5 kb to the right and 8.0 kb to the left of the HBV integration site did not show any homology to each other (Fig. 1C, bottom line). For example, the Hind